Procedia CIRP 97 (2021) 308–312

Contents lists available at ScienceDirect

Procedia CIRP

journal homepage: www.elsevier.com/locate/procir

Combining safety and speed in collaborative assembly systems – An approach to time optimal trajectories for collaborative robots

Rafael A. Rojas*, Manuel A. Ruiz Garcia, Luca Gualtieri, Erwin Rauch

Free University of Bozen-Bolzano, Faculty of Science and Technology, Piazza Unversità 1, Bozen-Bolzano 39100, Italy

ARTICLE INFO

Article history:
Received 30 September 2019
Revised 22 August 2020
Accepted 26 August 2020

Keywords:
Industry 4.0
Collaborative robotics
Trajectory planning
Assembly
Safety
Ergonomics

ABSTRACT

Human-robot interaction is a key enabling technology of Industry 4.0 and the prospected pervasiveness of robotics in industrial environments will be not possible without enabling them to safety interact with humans. Such a fact imposes a relevant constraints because the limits imposed by the actual technical deliverables entail strong requirements in the operational velocity of robots when sharing their workspace with humans. In this paper, we address the theoretical limits of velocity under the light of current state-of-the-art trajectory planning and normative requirements. The main goal is to find a methodology to plan safe trajectories without neglecting cognitive ergonomics and production efficiency aspects. We start by considering the set of trajectories which are optimal with respect to a cognitive criteria and give a suitable parametrization to it. Then we are able to formulate the safety requirements in terms of constraints in an optimization problem. Finally, experimental results are provided. This allow the identification of the preferable sets of possible motions which satisfy the operator psychological wellbeing and the assembly process performance by complying the safety requirements in terms of mechanical risk prevention.

1. Introduction

With the on-going trend towards Industry 4.0, all industries are increasingly relying on digitalization to become more competitive. Today, such a digitalization of the actual workspace is being partially achieved by the introduction of the so-called collaborative robots (*cobots*), a particular type of cyber-physical system (CPS) (Rojas and Garcia, 2020; Rojas et al., 2017).

Cobots are designed to achieve safe physical human-robot interaction (pHRI) (Gualtieri et al., 2020; ISO 10218-1:2011, 2011). Their main objective is to help operators to perform manual activities without exposing him or her to the safety risks that characterize traditional robots. The implementation of cobots is aimed to improve the performance of production systems and the work conditions of workers by matching typical machine strengths with human skills (Rojas et al., 2019). Collaborative systems can provide many advantages but also challenges in terms of physical human-robot interaction (HRI). In particular, combining safety with ergonomics is of major complexity.

However, it is worth noting that a cobot by itself cannot be considered save or collaborative without a risk analysis of its operation mode. Actually, a collaborative system is designed to interact with a human within a defined collaborative workspace where the main hazard category will be of mechanical type (ISO 10218-2:2011, 2011). This is because it is easier to identify possible unexpected contacts between the human and the robot in a delimited area. While collaborative robots present some inherent safety measures, as soon the cobot is integrated into a collaborative workspace and equipped with a custon end-effectors, such safety measures are rarely sufficient to ensure a safe operation mode.

To facilitate the identification of a cobot operation mode, the International Organisation for Standardization (ISO) has introduced 4 categories (ISO 10218-1:2011, 2011) aimed to implement mechanically safe installation of cobots, namely hand guiding, safety-rated monitored stop, speed and separation monitoring, and power and force limiting. Note that all of these operation modes largely rely on the robot's situational awareness capacity. In particular, safety-rated monitored stop and, speed and separation monitoring may require the implementation of a perceptive system in order to measure the relative position of the operator with respect to the robot.

It follows that a cobot as a single entity must provide the necessary interfaces to connect with other perception systems and/or

* Corresponding author.
E-mail address: rafael.rojas@unibz.it (R.A. Rojas).

https://doi.org/10.1016/j.procir.2020.08.003

a minimal degree self-awareness in order to be considered as such. In fact, several commercially available cobots provide the required features and tunable parameters to allow the integrator to implement out-of-the-box hand guiding and power and force limiting operation modes (ABB, 2018; ISO 10218-2:2011, 2011; Robots, 2017). It is also possible to implement a speed and separation monitoring operation mode without further implementation of perception systems. In fact, if the design of the collaborative workspace restricts the possible positions of the operator to a delimited area then the relative position of the operator with respect to the robot may be approximated according to a safety rated procedure.

In addition to the physical safety, other important topics have to be considered when designing and implementing a collaborative workspace. Recently, ergonomics and *psychological* safety has received attention in literature (Kokabe et al., 2008; Or et al., 2009), focusing on the subjective acceptance of the robot by its human partner. It this regard, it has been noted that smooth and predictable motions of the robot largely improve the operators psychical wellness (Arai et al., 2010; Lasota and Shah, 2015). In turns, it is possible improve the working environment in terms of pure trajectory planning.

Another key feature is an intuitive and simple way for teaching the robot a new task. Several commercially available cobots are endowed with a programming interface which operates under the hand-guiding ISO operation mode. Such a programming methodology consists in manually positioning and orienting the robot in a sequence of pertinent poses, called *waypoints*, so to define step by step the desired motion in terms of its geometrical path. As a result, such a programming scheme delegates the traditional difficulties of path planning to the robot's operator.

Among smooth motions that may enable psychological safety, minimum-jerk motions have gain attention as there is experimental evidence suggesting that humans move in that way (Flash and Hogan, 1985; Meirovitch et al., 2016; Oguz et al., 2018). Moreover, minimum-jerk trajectories reduce vibrations and wear in the robot's mechanics as well as the error during the trajectory tracking phase (Gasparetto and Zanotto, 2007). Considering that such a minimization principle may endow motions with the further advantage of familiarity to the operator (Rojas et al., 2019), we propose a trajectory planning technique to achieve both safer and faster collaborative robot behaviours on top of the classical hand-guiding programming technique by exploiting such a minimization principle.

One outstanding property of minimum-jerk trajectories is their optimality invariance under linear time-scaling, the largest widespread scaling technique among robotics applications (De Luca and Farina, 2002; Hollerbach, 1984). This implies that the execution time of such an optimal trajectory can be arbitrary and does not need to be defined as input to the optimization procedure. Despite, pure minimum-jerk trajectories -by design- do not minimize the length of the underlying trajectory path. Therefore, under certain circumstances, this may lead to an observable over-damped smoothness of the path's curvature, causing unexpected and difficult to predict overshoots on the resulting path.

To avoid the above issue, we propose the joint minimization of both the jerk and the speed along the path in terms of regularization the optimization problem. In complete analogy to Rojas et al. (2019, 2020), we directly apply the variational formalism to derive optimal trajectories providing a trade-off between jerk and speed minimization. Such a procedure differentiates from a theoretical perspective the current work with most of optimization approaches used in trajectory planning (Garcia et al., 2019; Gasparetto et al., 2012) such as methods based in Optimal Control Theory (Rojas and Carcaterra, 2018). The effectiveness of the approach is demonstrated empirically on a real collaborative assembly workspace.

2. Optimal trajectory planning

Following the same notation of Rojas et al. (2019), we describe the trajectory of the robot as a curve in the space $\mathbf{q} : J \longrightarrow \mathbb{R}^n$ in a fixed time interval $J = [0, T]$. Such a treatment allows to describe the motion in either the joint space, the Cartesian space or an specific task space. The different descriptions are achieved by choosing the dimension of the codomain of $\mathbf{q}$, denoted by n as desired.

As stated before, we will minimize a combination of the jerk (smoothness) and the arc length (speed). Such a combination is equivalent to combining psychological safety with speed and mechanical hazard in relation to ISO/TS 10218-1:2016 (2016). To provide a mathematically consistent combination of both we use convex combination governed by a regularization parameter $\alpha \in [0, 1]$. The limit values of such a parameter will represent the minimization of the jerk $\alpha = 0$ and the minimization of the speed $\alpha = 1$. Formally we are aimed to minimize

$$I(\mathbf{q}) = \int_0^T (1-\alpha)\|\dddot{\mathbf{q}}\|^2 + \alpha\|\dot{\mathbf{q}}\|^2 \, \mathrm{d}t \tag{1}$$

The optimal curve is subject to the condition of passing through a series of $N+1$ waypoints $\{\mathbf{q}_0, \mathbf{q}_1, \cdots, \mathbf{q}_N\}$ at a series of undefined time instants $\{t_0, t_1, \cdots, t_N\}$. $\mathbf{q}_0$ and $\mathbf{q}_N$ represents the first and last points of the trajectory, respectively, attained at the endpoints $t_0 = 0$ and $t_N = T$. These constraints can be then written as:

$$\mathbf{q}(t_i) = \mathbf{q}_i, \quad i = 0, \ldots, N. \tag{2}$$

Also, both the velocities and the accelerations at $\mathbf{q}_0$ and $\mathbf{q}_N$ are constrained as follows

$$\dot{\mathbf{q}}(t_0) = \dot{\mathbf{q}}_0, \quad \dot{\mathbf{q}}(t_N) = \dot{\mathbf{q}}_N, \quad \ddot{\mathbf{q}}(t_0) = \ddot{\mathbf{q}}_0, \quad \ddot{\mathbf{q}}(t_N) = \ddot{\mathbf{q}}_N. \tag{3}$$

It is worth noticing that constraints (3) may be extended so to include a desire velocity vector at every waypoint.

In complete analogy with Rojas et al. (2019), through the application of the variational formalism it is possible to obtain the following necessary conditions for the stationarity of (1) at $\mathbf{q}$:

$$\frac{\mathrm{d}^6\mathbf{q}}{\mathrm{d}\, t^6} + \frac{\alpha}{(1-\alpha)}\ddot{\mathbf{q}} = 0 \tag{4}$$

$$\mathbf{q} \in \mathcal{C}^4(\mathbb{R}, \mathbb{R}^n) \tag{5}$$

$$\left[\alpha\left(\tfrac{\mathrm{d}^5\mathbf{q}}{\mathrm{d}t^5}(t_i^+) - \tfrac{\mathrm{d}^5\mathbf{q}}{\mathrm{d}t^5}(t_i^-)\right) + (1-\alpha)\left(\ddot{\mathbf{q}}(t_i^+) - \ddot{\mathbf{q}}(t_i^-)\right)\right]^\top \dot{\mathbf{q}}(t_i) = 0. \tag{6}$$

The general solution of (4)–(6) may be easily written by introducing the set $J_0 = [-1, 1]$, the vector $\boldsymbol{\tau} \in \mathbb{R}^N$ with components $\tau_i = t_{i+1} - t_i$ and the family of linear dilations $s_i : J_i \longrightarrow J_0$ defined by

$$s_i(t) = 2\,\frac{t - t_i}{\tau_i} - 1. \tag{7}$$

Then, applying the transformation (7)–(4) we obtain that at each interval $J_i = [t_i, t_{i+1}]$ its solution is given by a linear combination of the following functions

$$\begin{aligned} B_{i0}(s) &= e^{k_i s}\cos(k_i s) \qquad B_{i1}(s) = e^{-k_i s}\cos(k_i s) \\ B_{i2}(s) &= e^{-k_i s}\sin(k_i s) \qquad B_{i3}(s) = e^{k_i s}\sin(k_i s) \\ B_{i4}(s) &= s \qquad B_{i5}(s) = 1, \end{aligned} \tag{8}$$

where

$$k_i = \frac{\tau_i\sqrt{2}}{4}\sqrt[4]{\frac{\alpha}{1-\alpha}}. \tag{9}$$

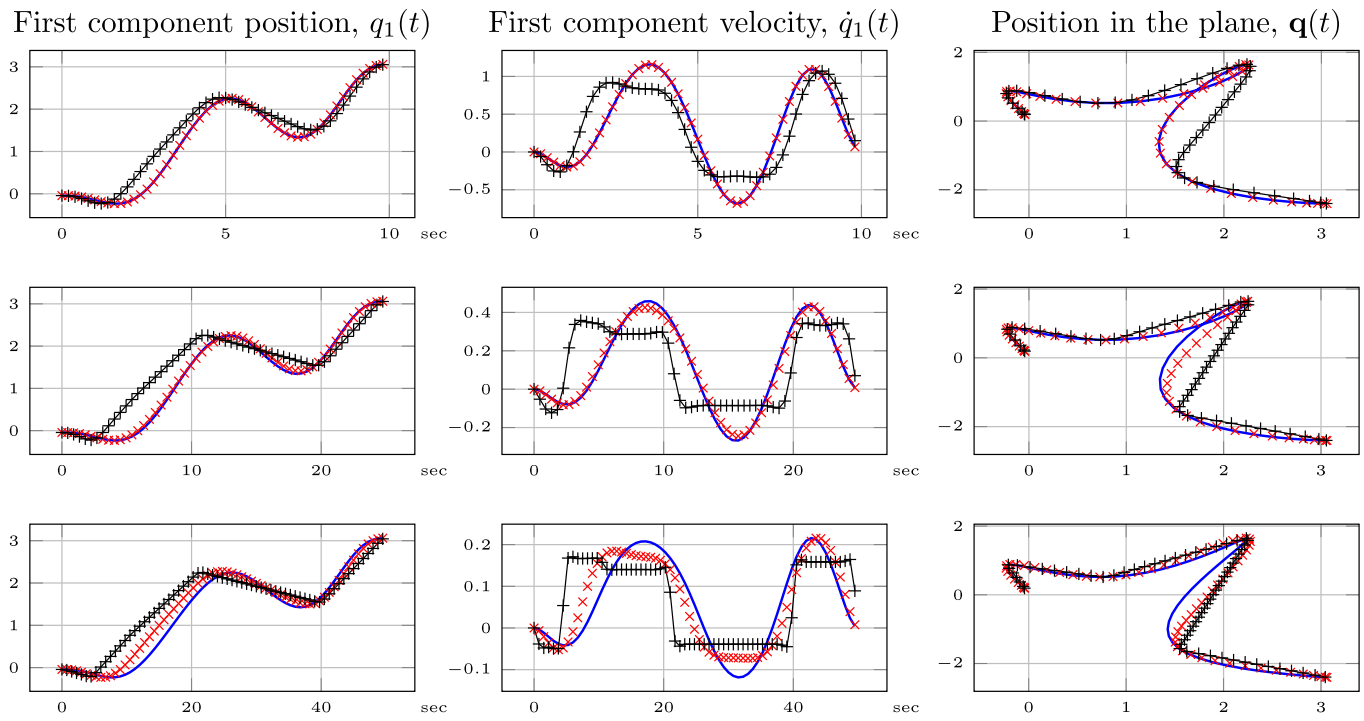

Fig. 1. Optimal trajectories with respect to (1) joining the waypoints in Table 1 for different execution times and values of α.

Table 1
Waypoints of the numerical example.

Waypoints	$\mathbf{q}_0$	$\mathbf{q}_1$	$\mathbf{q}_2$	$\mathbf{q}_3$	$\mathbf{q}_4$
Component 1	−0.043	−0.207	0.785	2.647	−1.600
Component 2	3.067	−1.205	2.647	1.012	1.00

This basis determines the representation of the i-component of the solution of (4) at the interval j as

$$q_i(t) = (\mathbf{y}_i^j)^\top \mathbf{B}_j\big(s_j(t)\big) \text{ if } t \in J_j, \tag{10}$$

where $\mathbf{B}$ represents the vector defined by stacking the basis $\{B_{ji}\}_{i=1}^6$ and $\mathbf{y}_i^j \in \mathbb{R}^6$.

We underline that the solution of form (10) represents a curve very similar to a traditional spline. In fact, meanwhile a traditional spline joints the waypoints constraints (2) and (3) using a polynomial of some degree, the form (10) joints them using a linear combination of the basis (8).

2.1. A numerical example

The minimization of (1) was implement following the numerical method presented in Rojas et al. (2019). However, in contrast with Rojas et al. (2019) the shape of the optimal of (1) does depend on the execution time T. To deepen in the relation of the trajectory with the execution time T and the parameter α we provide a numerical example with $n = 2$, $N = 3$ and the waypoints in Table 1. As such an example is done in a bidimensional space (a plane), each waypoint has two components. In Fig. 1 we present the time-evolution of the first component of the minimizers of (1) and the outcome path in the plane for different values of α and T.

Each row of Fig. 1 shows the behavior of the optimal of (1) for a different execution time. The values of T are 10.0, 25.0 and 50.0 for the first, second anf third row respectively. Each plot contains three different curves corresponding to $\alpha = 0.01$ (blue), $\alpha = 0.1$ (red) and $\alpha = 0.99$ (black). The first column of plots show the time evolution of the first-component position. The second column of plots show the time evolution of the first-component velocity. The third column of plots show the outcome path in the plane.

We can observe that as α becomes larger we are able to travel through the desired waypoints achieving smaller velocities for a fixed execution time. This fact is predictable from (1), as α regulates how much we minimize also the velocity. Following this idea, we regard α as a parameter of compromise between smoothness and maximum speed. If α is large, our trajectories will achieve smaller velocities but will be less smooth. If α is small, our trajectories will be smoother but they will achieve larger velocities. This fact makes α a parameter able to reduce the velocities achieved by the smooth collaborative motions presented in Rojas et al. (2019) for a given execution time.

Moreover, as T becomes larger the influence of α becomes stronger on the trajectory. In fact, we observe that the in the first row ($T = 10.0$) the black curve ($\alpha = 0.99$) is similar to the red curve ($\alpha = 0.1$) in the third row ($T = 50.0$). This implies that for a small times, the influence of the jerk in (1) is larger than the influence of the speed. As a consequence, when T is small even large values of α will be similar to minimum-jerk trajectories.

From the previous reasoning we draw that for a sufficiently large execution time T, minimum-jerk motions ($\alpha = 0$) will attain larger velocities in comparisons with other values of α. Our strategy to reduce the execution time of a smooth collaborative motion is to optimize (1) choosing a suitable value of α with a large execution time. Then we apply a linear scaling with a factor σ to the trajectory to achieve the maximum admissible velocity. In fact, we distinguish between the calculation execution time T in (1) and the effective execution time after the time scaling given by σT. Such a linear scaling will preserve the desired qualitative properties of the motion (De Luca and Farina, 2002; Hollerbach, 1984) i.e. its smoothness and the property of achieving smaller velocities than the minimum-jerk trajectory.

We underline that in contrast with the approach presented in Rojas et al. (2019), the optimality criteria (4)–(6) is not preserved after the scaling procedure. In fact, our strategy is not to imple-

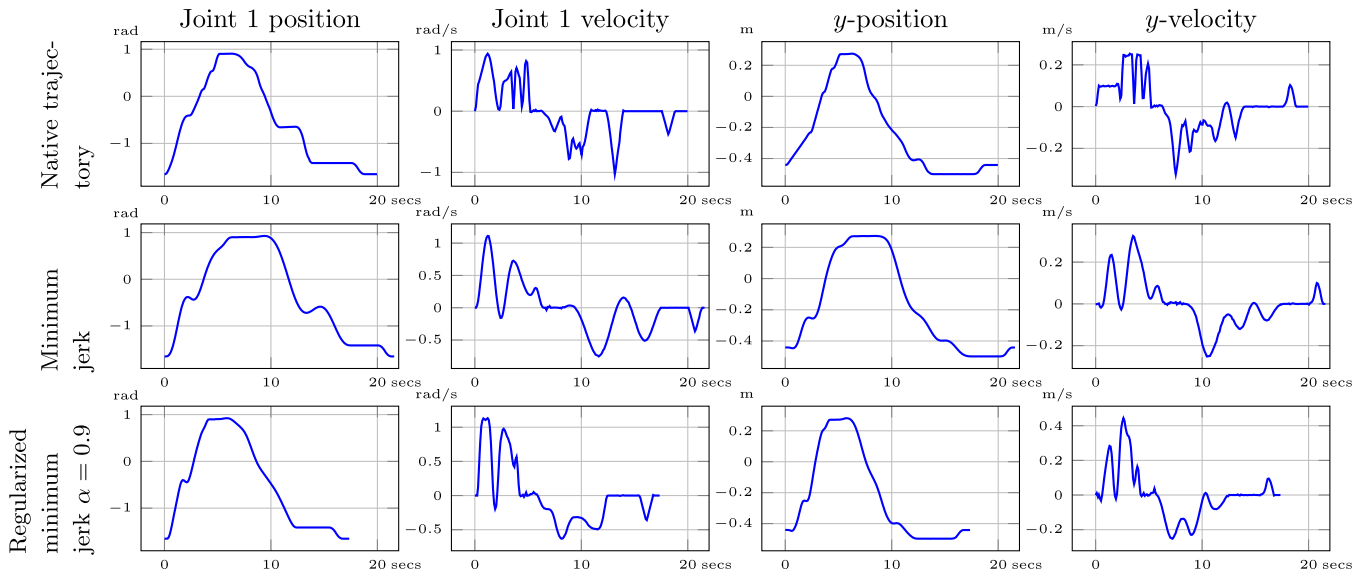

Fig. 2. Experimental results.

ment the optimum of (1) but use its optimal computed for arbitrary execution time T in order to obtain a trajectory which structurally achieves smaller velocities meanwhile preserving the smoothness of minimum-jerk trajectories.

3. Implementation

As a first test case, we focused on the transformation of a purely manual workstation for assembling pneumatic cylinders into a collaborative robotic cell at the Smart Mini Factory (SMF) lab (Gualtieri et al., 2018b). Following multipurpose focus of such a laboratory, the implementation of the current work is aimed to develop a meeting platform where research, learning and industry meet to allow a common and productive knowledge transfer. In particular, the SMF acts as a stakeholder in motion planning technologies capable to transfer such knowledge to local industries.

As described in Rojas et al. (2018) and Gualtieri et al. (2018a), the original workstation and its assembly cycle was analyzed to identify what critical issues could be improved by reconfiguring the cell with the introduction of a small collaborative robot. In this new station, the assembly components are organized *a priori* in a blister at predefined positions and the robot is only used to pass such components to the operator by following trajectories computed by joining a sequence of waypoints manually defined by the operator with the method described above.

Following the ISO standards 14121–2 (ISO T/R 14121-2:2012, 2012), 102018–2 (ISO 10218-2:2011, 2011) and TS-15066 (ISO/TS 10218-1:2016, 2016), we subdivide the station into collaborate and non-collaborative zones. Such a design allows to implement a mechanically safe collaborative workspace through a speed and separation monitoring operation mode. As described in Rojas et al. (2018), such a mechanically safe operation is possible constraining the speed of the robot's end-effector inside the collaborate zone to 250 mm/s in the direction of the operator.

The algorithm of our motion planner consist in the following steps

1. The operator move the robot to the desired sequence of waypoints.
2. The optimization of (1) is done using large values for T and α.
3. A linear scaling is applied to the trajectory obtained in the previous step in order to achieve the minimum execution time σT such that the maximum admissible speed is achieved. Note that this step achieves mechanical safety.

We can corroborate that this procedure will produce motions able to guarantee mechanical safety, less stress on the operator and fast motions. Mechanical safety is achieved in the sense of the TS-15066, thanks to the linear scaling applied in the third step which is also meant to achieve the mechanical feasibility of the motion.

The capability of this motions to induce less stress than other motions (e.g. trapezoidal velocity profiles) is guaranteed by its intrinsic smoothness, consequence of the property (5). Moreover, the term proportional to the jerk in (1) guarantees that depending on the chose of the parameter α we can achieve a certain level of similarity to human motions. However, the programmer can achieve smoother motions by choosing the smaller values of T and α in the step 2. We can conclude that these parameters may be used to choose a compromise between smoothness and speed.

Finally, the swiftness of the resulting motions with respect to minimum jerk motions is guaranteed by the minimization of the term proportional to the arc length in (1).

4. Experiment

Our experimental setup consists of a pick-and-pass task composed by two different trajectories executed in sequence. The first trajectory is for picking and the second for passing. We compared three different trajectory planners to achieve this task joining the same sequence of waypoints. Namely, we test the robot's embedded planner, a minimum jerk smooth collaborate planner and the one based on this work.

The experiment was realized using the UR3 lightweight robot. This is the smaller robot produced by Universal Robots, designed for both, assembly and workbench tasks, where the payload does not exceed 3 kg. It is a 6-axis anthropomorphic robot with an almost spherical workspace with a radius of 500 mm. The control scheme was implemented in its Mini-ITX PC and attached to its controller, using the URControl daemon. Moreover, a visual interface was made available into its Graphic User Interface called PolyScope in order to use its touch screen pendant for the trajectory planning.

Before presenting the comparisons between the different trajectory planning schemes, we underline that the build-in motion planner available in the robot is not capable of reproducing

our collaborative implementation of motion. The Universal Robots' planner provides a trapezoidal velocity profile trajectory defined by the absolute value of the maximum desired velocity of the end-effector without considering any particular direction. This implies that making the motion of the robot to a TS-15066 compliant with respect to the speed will penalize the motion also in the directions where no safety measure are required.

Fig. 2 depicts the experimental results. Note that the velocity in the direction of the operators does not exceed the mechanical safety limit of 250 mm/s. Each row describes the motion achieved by each planner. The first and the second columns show the time-evolution of the position and velocity of the first joint respectively. The third and the fourth columns show the time-evolution of the position and velocity of the end-effector of the robot in the direction of the operator. The trapezoidal velocity profile planner executes the task in 19.9 s. The minimum jerk planner executes the task in 21.5 s. The proposed planner executes the task in 17.3 s.

We remark that the main advantage of our proposed motions with respect to motions with trapezoidal velocity profile is its capabilty of bending smoothly at the waypoints. In fact, by its intrisec desing, trapezoidal velocity profiles need to stop at the corners of the planned path in order to achieve continuity of the motion. On the contrary, our proposed approach is able to generate paths which bend smoothly at the waypoints, avoiding sharp edges and allowing the motion to change direction without large variations of the acceleration.

5. Conclusions

This paper proposes a novel approach to reduce the execution time of collaborative motions. Focussed on SME environments we designed of physically safe motion focusing in the psychological aspect, preserving as much as possible the smoothness of the motion. In addition, such trajectories have the merit of preserving some of the advantages of minimum jerk motions.

As part of the solution we developed a new kind of spline-like curves able to joint waypoints smoothly. It can be seen that such curves are between a trapezoidal velocity profile curve and a fifth order spline. This new kind of curves may be implemented in different applications that have not been explored in this paper. However, further work is necessary in order to test the actual effectiveness of the presented approach with respect to the psychological relief and other important qualities of motion such a torque and consumed energy.

As a proof of concept, we presented an experimental setup and provide insights on the implementation of the proposed method. We achieved the reduction of the execution time of the task by a 13.1% with respect to the robot's default planner and by a 19.6% with respect the minimum jerk smooth collaborate planner.

The new approach makes the application of optimal smooth paths much more attractive. In fact, as the advantages of minimum-jerk motions may be outmatched by the time requirements of an application a cobot's integrator may abandon such kind of motions. Our approach has both benefits of reducing mental stress for the operator working with the cobot and achieving shooter execution times. Thus, this new approach has a high relevance for manufacturers of collaborative robots (e.g. for integration as a path option in the robot pendant software) as well as for users (e.g. as an online service for calculation of the optimal path and subsequent transfer to the robot). Thus, this new technology offers interesting business case options for exploitation and commercialization.

Declaration of Competing Interest

The authors declare that they have no known competing financial interests or personal relationships that could have appeared to influence the work reported in this paper.

The authors declare the following financial interests/personal relationships which may be considered as potential competing interests:

The authors do not have any kind of financial or personal relationship that may be considered as potential competing interest.

References

ABB, 2018. Operating Manual IRB 14000. Technical Report. ABB.

Arai, T., Kato, R., Fujita, M., 2010. Assessment of operator stress induced by robot collaboration in assembly. CIRP Ann. 59 (1), 5–8.

De Luca, A., Farina, R., 2002. Dynamic scaling of trajectories for robots with elastic joints. In: Proceedings 2002 IEEE International Conference on Robotics and Automation (Cat. No. 02CH37292), 3. IEEE, pp. 2436–2442.

Flash, T., Hogan, N., 1985. The coordination of arm movements: an experimentally confirmed mathematical model. J. Neurosci. 5 (7), 1688–1703.

Garcia, M.A.R., Rojas, R.A., Pirri, F., 2019. Object-centered teleoperation of mobile manipulators with remote center of motion constraint. IEEE Robot. Autom. Lett. 4 (2), 1745–1752.

Gasparetto, A., Boscariol, P., Lanzutti, A., Vidoni, R., 2012. Trajectory planning in robotics. Math. Comput. Sci. 6 (3), 269–279.

Gasparetto, A., Zanotto, V., 2007. A new method for smooth trajectory planning of robot manipulators. Mech. Mach. Theory 42 (4), 455–471.

Gualtieri, L., Rauch, E., Rojas, R., Vidoni, R., Matt, D.T., 2018. Application of axiomatic design for the design of a safe collaborative human-robot assembly workplace. In: MATEC Web of Conferences, 223. EDP Sciences, p. 01003.

Gualtieri, L., Rojas, R., Carabin, G., Palomba, I., Rauch, E., Vidoni, R., Matt, D.T., 2018. Advanced automation for SMES in the i4. 0 revolution: engineering education and employees training in the smart mini factory laboratory. In: 2018 IEEE International Conference on Industrial Engineering and Engineering Management (IEEM). IEEE, pp. 1111–1115.

Gualtieri, L., Rojas, R.A., Garcia, M.A.R., Rauch, E., Vidoni, R., 2020. Implementation of a laboratory case study for intuitive collaboration between man and machine in SME assembly. In: Industry 4.0 for SMEs, p. 335.

Hollerbach, J.M., 1984. Dynamic scaling of manipulator trajectories. J. Dyn. Syst. Meas.Control 106 (1), 102–106.

ISO 10218-1:2011, 2011. Robots and Robotic Devices – Safety Requirements for Industrial Robots – Part 1: Robots. Standard. International Organization for Standardization, Geneva, CH.

ISO 10218-2:2011, 2011. Robots and Robotic Devices – Safety Requirements for Industrial Robots – Part 2: Robot Systems and Integration. Standard. International Organization for Standardization, Geneva, CH.

ISO T/R 14121-2:2012, 2012. Safety of machinery – Risk assessment – Part 2: Practical guidance and examples of methods. Standard. International Organization for Standardization, Geneva, CH.

ISO/TS 10218-1:2016, 2016. Robots and Robotic Devices – Collaborative Robots. Technical Specification. International Organization for Standardization, Geneva, CH.

Kokabe, M., Shibata, S., Yamamoto, T., 2008. Modeling of handling motion reflecting emotional state and its application to robots. In: Proceedings of the SICE Annual Conference. IEEE, pp. 495–501.

Lasota, P.A., Shah, J.A., 2015. Analyzing the effects of human-aware motion planning on close-proximity human–robot collaboration. Hum. Factors 57 (1), 21–33.

Meirovitch, Y., Bennequin, D., Flash, T., 2016. Geometrical invariance and smoothness maximization for task-space movement generation. IEEE Trans. Robot. 32 (4), 837–853.

Oguz, O.S., Zhou, Z., Glasauer, S., Wollherr, D., 2018. An inverse optimal control approach to explain human arm reaching control based on multiple internal models. Sci. Rep. 8 (1), 5583.

Or, C.K., Duffy, V.G., Cheung, C.C., 2009. Perception of safe robot idle time in virtual reality and real industrial environments. Int. J. Ind. Ergon. 39 (5), 807–812.

Robots, U., 2017. User Manual UR3/CB3 Original Instructions. Technical Report. Universal Robots.

Rojas, R.A., Carcaterra, A., 2018. An approach to optimal semi-active control of vibration energy harvesting based on mems. Mech. Syst. Signal Process. 107, 291–316.

Rojas, R.A., Garcia, M.A.R., 2020. Implementation of industrial internet of things and cyber-physical systems in SMES for distributed and service-oriented control. In: Industry 4.0 for SMEs. Palgrave Macmillan, Cham, pp. 73–103.

Rojas, R.A., Rauch, E., Dallasega, P., Matt, D.T., 2018. Safe human-machine centered design of an assembly station in a learning factory environment. In: Proceedings of the 8th International Conference on Industrial Engineering and Operations Management.

Rojas, R.A., Rauch, E., Vidoni, R., Matt, D.T., 2017. Enabling connectivity of cyber-physical production systems: a conceptual framework. Procedia Manuf. 11, 822–829.

Rojas, R.A., Ruiz Garcia, M.A., Wehrle, E., Vidoni, R., 2019. A variational approach to minimum-jerk trajectories for psychological safety in collaborative assembly stations. IEEE Robot. Autom. Lett. 4 (2), 823–829.

Rojas, R.A., Wehrle, E., Vidoni, R., 2020. A multicriteria motion planning approach for combining smoothness and speed in collaborative assembly systems. Appl. Sci. 10 (15), 5086.